Radical Cage Effects in the Photochemical Degradation of Polymers: In-Cage Trapping of Photochemically Generated Radical Cage Pairs in Polymer Model Compounds

Jonathan L. Male,[†] Myungok Yoon,[†] Anne G. Glenn,[‡] T. J. R. Weakley,[†] and David R. Tyler*,[†]

Department of Chemistry, University of Oregon, Eugene, Oregon 97403, and Department of Chemistry, Guilford College, 5800 W. Friendly Avenue, Greensboro, North Carolina 27410

Received January 20, 1999; Revised Manuscript Received April 19, 1999

ABSTRACT: This study explored the origins of the observation that the overall quantum yields for polymer photodegradation depend on the polymer chain length. The $(CH_3(CH_2)_nC(O)NHCH_2CH_2Cp)_2Mo_2(CO)_6$ (n = 3, 8, 13, 18) complexes (**1**−**1**−**4**−**4**) were synthesized and used as model complexes for the study. As is common for metal−metal bonded complexes of this type, irradiation of these molecules cleaved the metal−metal bonds and formed free radicals via the intermediate formation of a radical cage pair. Studies on previous model complexes showed that the quantum yields for degradation decreased as the chain length of the complex increased. The decrease in quantum efficiency was partially attributed to an increase in the radical cage effect as the chain length increased. Surprisingly, however, the overall quantum yields and cage effects for complexes **1**−**1**−**4**−**4** did not vary significantly with chain length. The similarity in the quantum yields and in the cage effects for these molecules is attributed to an internal trapping reaction of the metal radicals in the solvent cage by the H atom of the amide group. The resulting Mo···(H)−N agostic interaction forms a six-membered ring. The trapping reaction takes place by segmental rotation of the metal-containing end of the radical chain; the rate of this motion is independent of the chain length, and thus differences in the cage effects and the overall quantum yields will be diminished for the four molecules. The X-ray crystal structure of the $(CH_3(CH_2)_3C(O)NHCH_2CH_2Cp)_2Mo_2(CO)_6$ molecule is also reported.

Introduction

Photochemically reactive polymers[1−3] are of considerable interest because they are useful as degradable plastics,[4] photoresists,[5−9] biomedical materials, and precursors to ceramic materials.[5−7,10−13] To expand the repertoire of photodegradable polymers, we have been developing a new class of polymers that contain metal−metal bonded organometallic dimers interspersed along the polymer backbone.[14−16] These polymers are photodegradable because the metal−metal bonds can be cleaved with visible light and the resulting metal radicals captured with oxygen or other traps (Scheme 1).[17]

In a recent paper, we showed that the overall quantum yields for the degradation of these polymers and model complexes varied as a function of molecular weight and size.[15] This is an expected result because the quantum yields for the photodegradation of polymers are generally dependent on the chain length. For example, Guillet showed that overall quantum yields for the Norrish type I degradations of various model aliphatic ketones decreased as a function of chain length.[18] Reasons for the dependence of the quantum yields on the chain length have been a matter of considerable interest and speculation.[19] It is generally hypothesized[18] that the dependence is attributable either to changes in ϕ_{pair} (the quantum yield for the formation of the radical cage pair; Scheme 2) or to changes in the "cage recombination efficiency" as the chain length is varied.[20] (The "cage recombination efficiency" (denoted as F_c) is defined as the ratio of the rate constant for cage recombination to the sum of the rate constants for all competing cage processes. The F_c value for a photochemically formed cage pair does not necessarily equal F_c for the same cage pair formed by thermolysis or by diffusional collision of two free radicals.[21] To differentiate these cases, the photochemical cage efficiency will be denoted F_{cP} and the associated rate constants as k_{cP} and k_{dP}. In the photolysis reaction in Scheme 2, $F_{cP} = k_{cP}/(k_{cP} + k_{dP})$.)

Scheme 1. Photochemical Degradation of a Polymer with Metal−Metal Bonds along Its Backbone

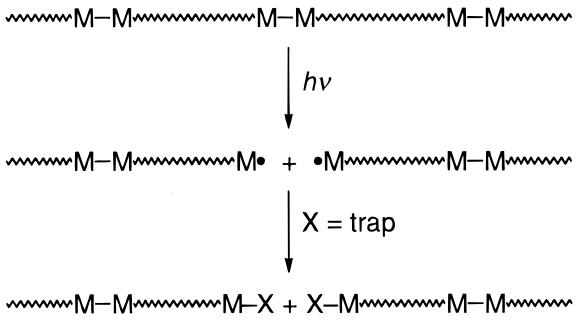

Scheme 2. Reaction Scheme for Metal−Metal Bond Photolysis

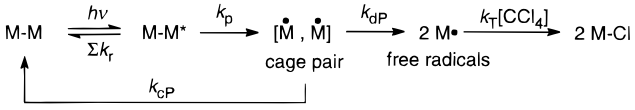

M = metal containing fragment
$F_{cP} = k_{cP}/(k_{cP} + k_{dP})$; $\phi_{pair} = k_p/(k_p + \Sigma k_r)$

[†] University of Oregon.
[‡] Guilford College.
* Corresponding author.

10.1021/ma990074z CCC: $18.00 © 1999 American Chemical Society
Published on Web 05/27/1999

To gain greater insight into the role that ϕ_{pair} and F_{cP} play in controlling the degradation of polymers, we synthesized the series of polymer model complexes $(CpCH_2CH_2OSiR_3)_2Mo_2(CO)_6$ (R = Me, *i*-Pr, *n*-Pr, *n*-Hx) and determined ϕ_{pair} and F_{cP} for each.[22] (These molecules will henceforth be referred to as the "silylated" molecules in this paper.)

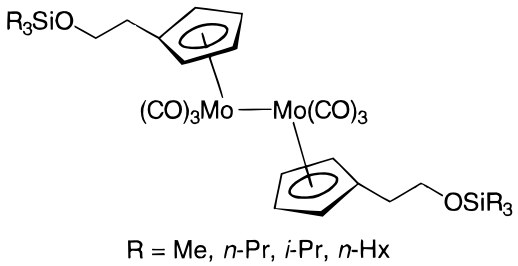

R = Me, *n*-Pr, *i*-Pr, *n*-Hx

As reported in this journal,[22a] the overall quantum yields for these molecules decreased as the chain lengths increased (as was the case with Guillet's straight-chain aliphatic symmetric ketones[18]). Furthermore, the cage recombination efficiencies increased as the chain lengths increased. Thus, the decrease in the overall quantum yield with increasing chain length can be at least partially attributed to an increase in F_{cP}.[23,24]

To study the generality of the results obtained with the silylated molecules, we synthesized the model complexes $(CH_3(CH_2)_nC(O)NHCH_2CH_2Cp)_2Mo_2(CO)_6$ (*n* = 3, 8, 13, 18) (**1**−**1**−**4**−**4)** and determined ϕ_{pair} and F_{cP} for each. (The unconventional numerical nomenclature assigned to these dimers is used to facilitate discussion of their cage pairs. Thus, the radical cage pair for dimer **1**−**1** becomes [**1**•, •**1**], etc.) This paper reports the results of our study and the implications they have for the photochemical cleavage of polymer backbones.

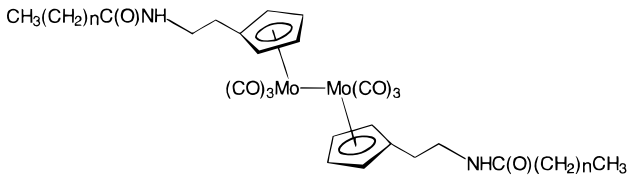

1-1, n = 3; **2-2**, n = 8; **3-3**, n = 13; **4-4**, n = 18

Results and Discussion

The Method for Measuring ϕ_{pair} and F_{cP}. The technique for obtaining F_{cP} and ϕ_{pair} values has been described thoroughly in previous papers.[22,25] In short, these values are obtained by extracting them from overall quantum yield measurements of the photoreactions with CCl_4 (a metal-radical trap) as a function of solvent system viscosity (eq 1).

$$(RCp)_2Mo_2(CO)_6 \xrightarrow[CCl_4,\ THF/tetraglyme]{h\nu(546\ nm)} 2(RCp)Mo(CO)_3Cl + [2CCl_3] \quad (1)$$

The solvent system used in this study was a mixture of THF, tetraglyme, and CCl_4 (≈2 M). The viscosity was varied by changing the fraction of tetraglyme in the mixture.[26,27] With a sufficiently high concentration of CCl_4, all of the radicals that escape the cage will form the $(CpR)Mo(CO)_3Cl$ product.[17,22,30] Under these conditions, the overall quantum yield for disappearance of $(CpR)_2Mo_2(CO)_6$ is given by eq 2, where ϕ_{pair} is the quantum yield for formation of the cage pair [$\phi_{pair} = k_P/(k_P + \sum k_r)$] and $(1 - F_{cP})$ is the fraction of radical pairs that escape the cage (and which are then trapped by CCl_4).

Scheme 3. Synthesis of Molecules 1−1 to 4−4

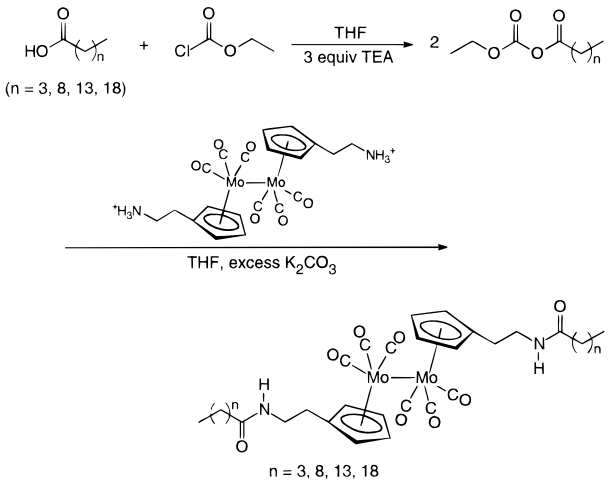

$$\Phi_{obsd} = \phi_{pair}[k_{dP}/(k_{cP} + k_{dP})] = \phi_{pair}[1 - F_{cP}] \quad (2)$$

Rearrangement of eq 2 yields eq 3, from which it is clear that k_{cP}/k_{dP} (and in turn F_{cP}) can be calculated if ϕ_{pair} and Φ_{obsd} are known.[22,25] Because Φ_{obsd} can be measured, the problem of determining F_{cP} thus becomes one of determining ϕ_{pair}.

$$1/\Phi_{obsd} = [1/\phi_{pair}][1 + k_{cP}/k_{dP}] \quad (3)$$

To obtain ϕ_{pair}, $1/\Phi_{obsd}$ was plotted as a function of viscosity. If ϕ_{pair} is assumed to be independent of viscosity for a particular solvent system, then the *y*-intercept of this plot is equal to the reciprocal of ϕ_{pair}.[31,32] This last statement is shown by eq 3: the second term on the right-hand side contains a viscosity dependence such that k_{cP}/k_{dP} becomes much smaller than one as the viscosity approaches zero. Thus, at zero viscosity (infinite fluidity), Φ_{obsd} will equal ϕ_{pair}.

Synthesis. Molecules **1**−**1** to **4**−**4** were synthesized by the route shown in Scheme 3.[16] The molecules were obtained rigorously pure by repeated filtrations and recrystallizations from hexanes. The $-CH_2CH_2-$ spacer was specifically incorporated into these molecules to isolate the Mo−Mo chromophore from any electronic changes caused by varying the side chains on the Cp rings.[33] In fact, this strategy worked because the electronic spectra of the four molecules are essentially identical.[33] This result is important because it suggests that changes in the photophysical parameters will be caused only by differences in the lengths of the side chains and not by electronic differences in the metal−metal bond chromophores.

Molecular Structures. The molecular structure of the **1**−**1** molecule was confirmed by X-ray crystallography (Figure 1). As expected for a polyamide, intermolecular hydrogen bonding occurs in the solid state. (The solution-phase IR and NMR spectra, however, show no evidence of intermolecular H-bonding.) The bond lengths and angles in the $Cp_2Mo_2(CO)_6$ core are essentially the same as those in related molecules containing the $Cp_2Mo_2(CO)_6$ unit.[34] In particular, the Mo−Mo bond length in **1**−**1** (3.225(4) Å) is essentially

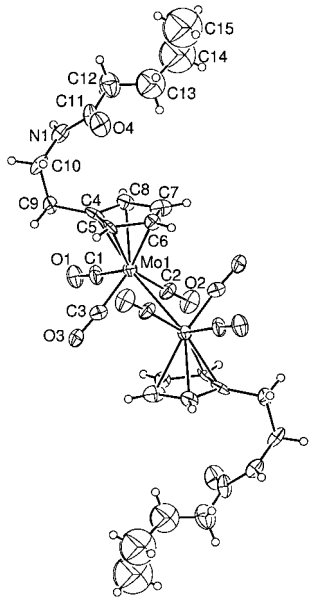

Figure 1. X-ray crystal structure of the $[(\eta^5\text{-}C_5H_4(CH_2)_2N(H)C(O)(CH_2)_3CH_3]_2Mo_2(CO)_6$ (**1**−**1**) molecule.

identical to those in $(MeCp)_2Mo_2(CO)_6$ (3.220(1) Å), $Cp_2Mo_2(CO)_6$ (3.235(1) Å), $(CpCH_2CH_2OSiMe_3)_2Mo_2(CO)_6$ (3.219(1) Å), and $(CpCH_2CH_2OH)_2Mo_2(CO)_6$ (3.211(1) Å).[34] This fact again suggests that the Mo−Mo bond is not significantly perturbed by the change in the side chain and that the Mo−Mo bond energies are essentially the same. Because the infrared, electronic absorption, and NMR spectroscopic data for the other model complexes are similar to those of complex **1**−**1**, the molecules are suggested to be structurally, as well as electronically, similar.

Chain Length Effects on the Quantum Yields, F_{cP}, and ϕ_{pair}. Using the method outlined above,[22,25] F_{cP} and ϕ_{pair} values for complexes **1**−**1** to **4**−**4** were obtained by measuring the overall quantum yields (Φ_{obsd}) for their reactions with CCl_4 in THF/tetraglyme as a function of viscosity (eq 1).[25] The overall quantum yields as a function of viscosity are shown in Figure 2 for the four dimers, the F_{cP} values are shown in Figure 3, and the ϕ_{pair} values are listed in Table 1. *Note that, within experimental error, at any given viscosity the overall quantum yields are equal, the ϕ_{pair} values are essentially equal, and the F_{cP} values show very little difference from each other.* These results are in stark contrast to our results reported earlier with the $(R_3SiOCH_2CH_2Cp)_2Mo_2(CO)_6$ (R = Me, *i*-Pr, *n*-Pr, *n*-Hx) molecules.[22] As mentioned in the Introduction, the overall quantum yields for these latter molecules were not constant as a function of chain length, but rather decreased as the chain length increased. Likewise, their ϕ_{pair} values decreased as the chain length increased,[35] and F_{cP} increased with increasing length of the substituent on the Cp ligand.[22] (In fact, the value of $F_{cP}^{-1} - 1$ was shown to be linearly proportional to $m^{1/2}/r^2$.[22]) For help in seeing that the differences in Φ_{obsd} and F_{cP} between the **1**−**1**, **2**−**2**, **3**−**3**, and **4**−**4** molecules are small, it is useful to compare Figures 1 and 2 to the analogous figures for the silylated molecules in ref 22. The differences are easily noted in this prior work.

Why are Φ_{obsd}, F_{cP}, and ϕ_{pair} essentially independent of chain length for **1**−**1** to **4**−**4**, yet dependent on the chain length in the case of the silylated molecules? As previously discussed, the pathway in Scheme 2 predicts

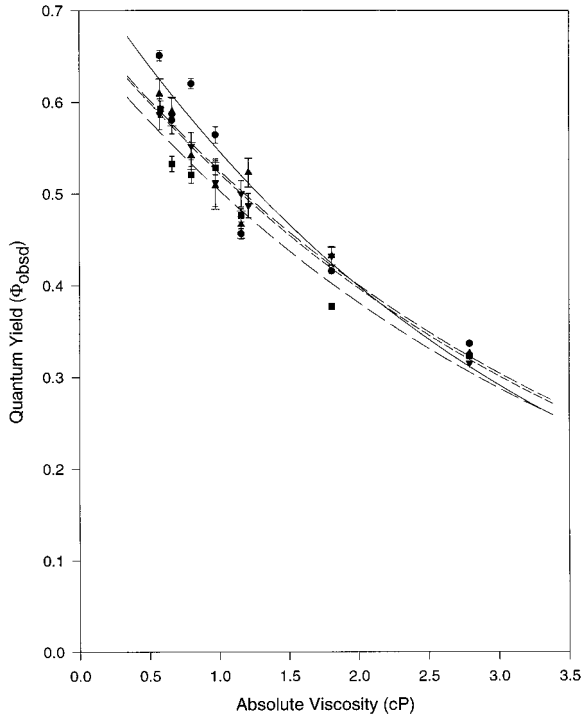

Figure 2. Plots of Φ_{obsd} vs viscosity for the photochemical reaction (λ = 546 nm) of molecules **1**−**1** (●), **2**−**2** (■), **3**−**3** (▲), and **4**−**4** (▼) with CCl_4 (≈2 M) at 23 ± 1 °C in THF/tetraglyme. All error bars represent ±1 σ.

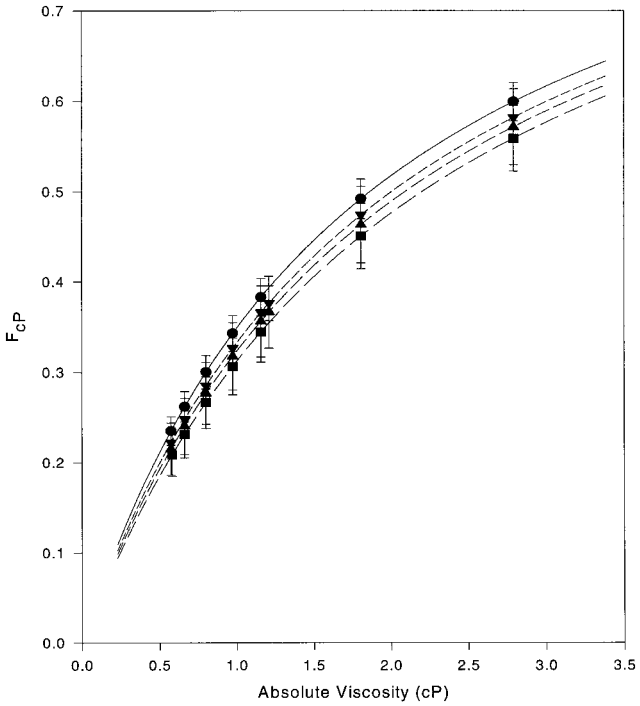

Figure 3. Plots of F_{cP} vs viscosity for cage pairs [**1**•,•**1**] (●), [**2**•,•**2**] (■), [**3**•,•**3**] (▲), and [**4**•,•**4**] (▼) at 23 ± 1 °C in THF/tetraglyme. All error bars represent ±1 σ.

that F_{cP} and Φ_{obsd} should vary with the mass and size of the radical. Because no such dependence was found, the implication is that Scheme 2 is incomplete for describing the reactivity of **1**−**1** to **4**−**4**. It is suggested, therefore, that the additional step in eq 4 must be added to the scheme in the case of molecules **1**−**1** to **4**−**4**. This new step involves segmental motion of the metal-containing end of the radical in the cage pair to form an agostic[36] Mo···H(N) bond. (The term "agostic" is used

Table 1. Selected Spectroscopic Data and Photochemical Results

compound	ϵ^a	$\phi_{pair}{}^b$	$k_c/k_d°$
$[(CH_3(CH_2)_3C(O)NHCH_2CH_2Cp)_2Mo_2(CO)_6$	1350 ± 20	0.82 ± 0.03	0.307 ± 0.027
$[(CH_3(CH_2)_8C(O)NHCH_2CH_2Cp)_2Mo_2(CO)_6$	1360 ± 30	0.72 ± 0.04	0.260 ± 0.038
$[(CH_3(CH_2)_{13}C(O)NHCH_2CH_2Cp)_2Mo_2(CO)_6$	1340 ± 60	0.77 ± 0.04	0.274 ± 0.046
$[(CH_3(CH_2)_{18}C(O)NHCH_2CH_2Cp)_2Mo_2(CO)_6$	1300 ± 60	0.78 ± 0.02	0.286 ± 0.023

[a] Extinction coefficient ($M^{-1}cm^{-1}$) in THF at 546 nm. [b] For comparison, the ϕ_{pair} values for $(R_3SiOCH_2CH_2Cp)_2Mo_2(CO)_6$ in THF were R = Me, 0.77 ± 0.05; R = *n*-Hx, 0.83 ± 0.04.

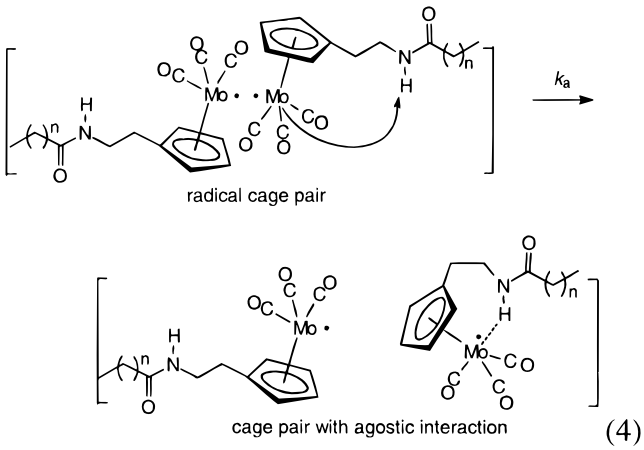

(4)

to describe the interaction in which a hydrogen atom is covalently bonded simultaneously to both a ligand atom and to a transition-metal atom.[36] The ligand atom is typically a carbon atom, but as discussed below many examples are now known where the ligand atom is nitrogen.) If the rate of formation of the agostic species is independent of the radical chain length (a reasonable assumption because segmental motion of the same molecular unit is required to form the agostic intermediate) and if it is formed irreversibly,[37] then the differences in the F_{cP} values will be diminished. (The basis for this statement is as follows. If the rate constant for the formation of the agostic intermediate is called k_a, then $F_{cP} = k_c/(k_c + k_d + k_a)$. Because k_a is assumed to be invariant with radical chain length, its presence in the denominator will mollify differences in the F_{cP} values based on the equation where $F_{cP} = k_c/(k_c + k_d)$. Although differences in F_{cP} are still expected, we suggest they are comparable to the experimental errors in the measurements and hence essentially indiscernible in a comparison of the four compounds.) In summary, it is suggested that the differences in the *physical* attributes of the radicals are mollified by a common *in-cage chemical reaction* that occurs at the same rate in each radical pair. The complete suggested reaction scheme is shown in Figure 4.

Semiempirical molecular mechanics calculations support the proposed agostic interaction. Thus, energy minimization calculations on the $[(CH_3(CH_2)_3C(O)NHCH_2CH_2Cp)(CO)_3Mo^•]$ radical using the PM3(TM) method converge on a structure with a Mo···H−N interaction like the one shown in eq 4 and Figure 4. Although once considered rare, many M···H−N agostic interactions are now known. Crabtree has compiled a list of these molecules and discussed their chemistry.[38] His review cites a typical M···H bond length of about 2.5 Å, which compares favorably with our calculated value of 2.43 Å in the $[(CH_3(CH_2)_3C(O)NHCH_2CH_2Cp)(CO)_3Mo^•]$ radical. It is also noted that analogues to the "tethered" interaction of the amide side chain that forms the agostic intermediate are well-known in the chemistry of metal radicals with Cp ligands. An example of this chemistry is shown in eq 5.[39] Further examples are cited in ref 39.

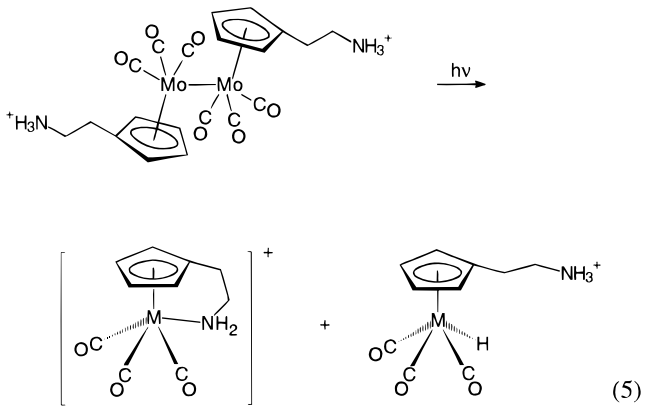

(5)

Additional evidence for the proposed agostic interaction comes from molecules that are incapable of forming an agostic Mo···H−N interaction. The k_a step does not exist for such molecules, and consequently they should show variations in their F_{cP} values. The silylated molecules fall in this category, and as discussed above, silylated molecules with different sizes do in fact have different F_{cP} and Φ_{obsd} values.[22]

An alternative explanation for how the k_a step equalizes the F_{cP} values in molecules **1**−**1** to **4**−**4** is the following. Note that one consequence of forming the agostic intermediate is to prolong the lifetime of the cage pair because recombination of the radicals is inhibited when at least one of them is "internally trapped" as an agostic species. Another consequence is the formation of a void between the radicals, formed by the segmental motion of the metal-containing end of the radical in the agostic bond-forming step. Because the cage pair is relatively long-lived, solvent molecules will move to fill the void (probably simultaneously with the segmental motion), which in essence results in the formation of two free radicals. No translational diffusional movement of the radicals in the agostic cage pair was required to form these free radicals, and hence there will be no dependence on the mass, size, or shape of the radicals. Consequently, F_{cP} will be independent of these parameters.

To conclude this section, it is noted that the equivalent ϕ_{pair} values in **1**−**1** to **4**−**4** seem logical because all of the molecules were designed with the $-CH_2CH_2-$ spacer as an electronic insulator between the side chains and the Cp rings. Because changes in ϕ_{pair} (in a common solvent) are caused by electronic changes in the molecules, the constant ϕ_{pair} values would seem to indicate a constant electronic environment for the Mo−Mo chromophore, as planned. Finally, note that because the ϕ_{pair} and F_{cP} values for molecules **1**−**1** to **4**−**4** are essentially equivalent, the overall quantum yields (Φ_{obsd}) will also be essentially the same (see eq 2).

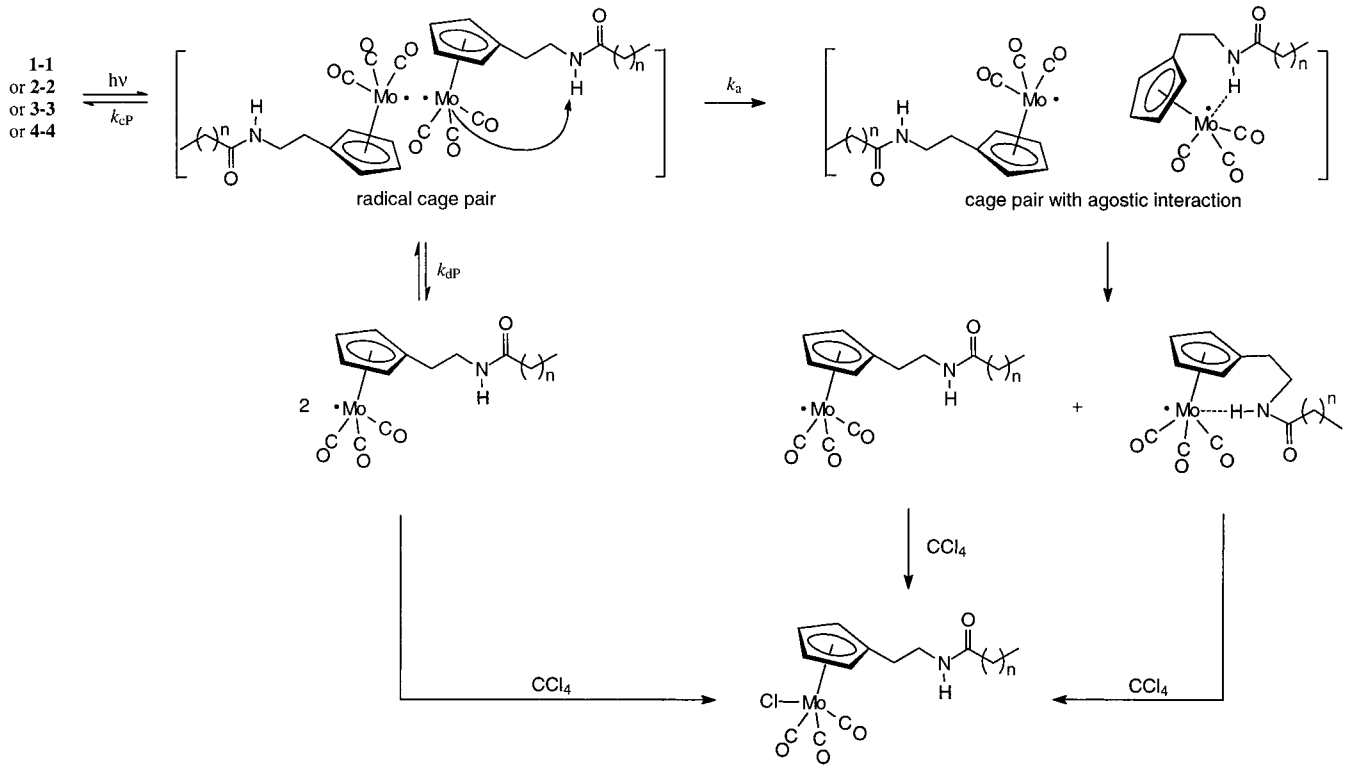

Figure 4. Proposed mechanism for the photochemical reactions of dimers **1**−**1** to **4**−**4**. Capture of the radicals with CCl_4 (as in Scheme 2) occurs after their separation to form free radicals in the k_d step. Rapid in-cage trapping diminishes differences in the F_{cP} values caused by differences in radical mass and size.

Table 2. Mass and Volume Data for the Radicals

radical	molec wt, g mol^{-1}	static molec vol,[a] Å^3	longest molec axis,[a] Å
$(CpCH_2CH_2NHCO(CH_2)_3CH_3)Mo(CO)_3$	372	202	15.68
$(CpCH_2CH_2OSiMe_3)Mo(CO)_3$	361	185	12.23
$(CpCH_2CH_2NHCO(CH_2)_8CH_3)Mo(CO)_3$	442	272	21.95
$(CpCH_2CH_2OSi(i\text{-}Pr)_3)Mo(CO)_3$	445	270	13.37
$(CpCH_2CH_2NHCO(CH_2)_{13}CH_3)Mo(CO)_3$	513	344	28.22
$(CpCH_2CH_2OSi(n\text{-}Pr)_3)Mo(CO)_3$	445	272	14.68
$(CpCH_2CH_2NHCO(CH_2)_{18}CH_3)Mo(CO)_3$	583	414	34.49
$(CpCH_2CH_2OSi(n\text{-}Hx)_3)Mo(CO)_3$	571	397	18.38

[a] The static volume can be viewed as a minimum value[55] while an isotropic rotation about the longest axis can be viewed as generating a maximum volume.

Other Explanations. Several other factors could account for the essentially equivalent Φ_{obsd}, ϕ_{pair}, and F_{cP} values in molecules **1**−**1** to **4**−**4**. One possible explanation involves the opposing effects of increased mass and volume on the cage effect. In his mathematical description of the cage effect, Noyes predicted that the cage effect will increase as radical size increases and as radical mass decreases.[40] Specifically, he predicted that the ratio k_d/k_c is proportional to $m^{1/2}/r^2$, where r is the radius of the radical and m is the mass.[21a,41] Mass and size data for the **1**$^{\bullet}$−**4**$^{\bullet}$ radicals (and, for comparison, the silylated radicals) are given in Table 2. Examination of these data shows that, as the radical chain length increases, the increase in size more than offsets the increase in mass. Thus, the cage effect should increase as the chain length of the radicals increases along the series **1**−**1** to **4**−**4**; offsetting mass and steric effects are therefore not the reason why these molecules behave similarly.

Another alternative explanation is again based on the notion that rotational diffusion (caused by segmental motion) is primarily responsible for diffusional separation of the two radical ends of the chains (as opposed to translational diffusion):[42]

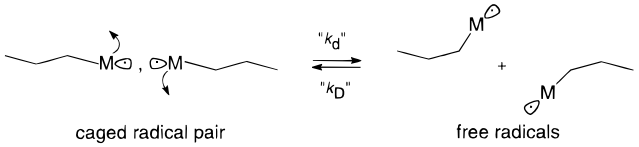

If such is the case, then, once a certain chain length is reached, additional chain length will not impact the segmental motion of the radical end. It would have to be argued that the model complexes used in this study had the required minimum chain length, and the cage effect was therefore constant for all the radical pairs. If this explanation is correct, then the $[(RCp)(CO)_3Mo^{\bullet}, {}^{\bullet}Mo(CO)_3(CpR)]$ (R = $CH_2CH_2OSi(n\text{-}Pr)_3$) and $[(RCp)(CO)_3Mo^{\bullet}, {}^{\bullet}Mo(CO)_3(CpR)]$ (R = $CH_2CH_2OSi(n\text{-}Hx)_3$) cage pairs should probably also exhibit limiting behavior because their net chain lengths are comparable to those of the molecules used in this study. In fact, however, the Φ_{obsd}, ϕ_{pair}, and F_{cP} values for these two silylated molecules are different,[22] a result that is hard to rationalize on the basis of this alternative explanation.

Key Conclusions and Insights. Radical pairs generated by photolysis of molecules **1**−**1** to **4**−**4** have constant cage recombination efficiencies, F_{cP}. Likewise,

the overall quantum yields for disappearance (Φ_{obsd}) of these dimers in CCl_4 were constant at all viscosities studied, and the ϕ_{pair} values were constant. These results were unexpected because previous work established that the mass and size of the radicals in a cage pair influenced F_{cP} according to the relationship $k_d/k_c \propto \text{mass}^{1/2}/\text{radius}^2$. It is proposed that F_{cP} is constant in the case of **1**−**1** to **4**−**4** because the amide functional group can interact with the metal-centered radical to form an agostic Mo···(H)−N bond. This interaction can take place by segmental rotation of the metal-containing end of the radical chain; the rate of this motion should be independent of the chain length, and thus the differences in F_{cP} will be diminished.

The work presented here shows that one strategy for effecting in-cage trapping of radical cage pairs is to "tether" the radical trapping agent to the radical. Intramolecular reactions are generally fast (especially chelating ring-closure reactions to form six-membered rings), and they can apparently compete with recombination of the radicals and diffusion out of the cage.

A direct test of the explanation presented above is to replace the H atom in the amide functional group with, say, a methyl group. Efforts are underway in our laboratory to prepare these materials.

Experimental Section

All manipulations were carried out in the absence of water and atmospheric oxygen using standard Schlenk line and drybox techniques.

Materials and Reagents. Molybdenum hexacarbonyl (Aldrich), 2-bromoethylamine hydrobromide (Aldrich), and *n*-butyllithium in cyclohexane (Aldrich) were used without further purification. THF (Fisher), hexanes (Baker), and ether (Fisher) were distilled from potassium benzophenone ketyl under nitrogen. Tetraglyme (tetraethylene glycol dimethyl ether, Aldrich) was distilled from Na−K alloy under reduced pressure.[43] C_6D_6 (Cambridge Isotope) and $CDC1_3$ (Cambridge Isotope) were distilled from Na−K alloy and P_2O_5, respectively, under nitrogen. DMSO-d_6 (Cambridge Isotope) was distilled from CaH_2 under reduced pressure. The radical trap $CC1_4$ (Fisher) was distilled twice from P_2O_5 and passed through a column of dry basic alumina. All solvents for quantum yield measurements were degassed by repeated freeze−pump−thaw cycles and stored in amber bottles under nitrogen prior to use. Ethyl chloroformate, valeric acid, capric acid, pentadecanoic acid, and eicosanoic acid (all from Fisher) were degassed by two freeze−pump−thaw cycles. Dicyclopentadiene (Aldrich) was cracked into an ice bath immediately prior to use.

Instrumentation and Procedures. Infrared spectra were recorded on a Nicolet Magna 550 FT-IR spectrometer with OMNIC software. Samples were prepared as either KBr pellets or as solutions in CaF_2 cells (path length 0.109 mm). UV−vis spectra were recorded with either a Perkin-Elmer Lambda 6 UV−vis spectrophotometer or a Beckman DU UV−vis spectrophotometer. All UV−vis spectrophotometers were calibrated with holmium oxide and neutral density filters. NMR spectra were collected on a Varian Unity/Inova 300 spectrometer at an operating frequency of 300 and 75 MHz for ^1H and ^{13}C nuclei, respectively. Elemental analyses were performed by E + R Microanalytical Laboratory, Inc., Corona, NY.

Overall quantum yields ($\lambda = 546$ nm) were determined with an Oriel Merlin system equipped with an Oriel 200 W high-pressure mercury arc lamp.[44] The silicon photodiode in the Merlin system was calibrated with Aberchrome 540[45] (irradiation at 546 nm and monitoring the drop in absorbance at 494 nm all at 23 ± 1 °C). Concerns over the use of Aberchrome 540 have recently arisen upon irradiation at ∼366 nm;[46] therefore, the calibration was also verified with Reineckate's salt.[47]

The mixed solvent systems were prepared in a darkened drybox. All solutions were 20% (v/v) $CC1_4$ (≈2 M) and with varying ratios of THF and tetraglyme (from 0 to 80 vol % tetraglyme). Absolute viscosities of the solutions were determined from the densities and kinematic viscosities of the solutions, which were measured at 23 ± 1 °C with calibrated Cannon-Fenske viscometers.

The bootstrapping technique was executed using the Bootstrap library (obtained from the Carnegie-Mellon University statistics archive)[48] and Splus software, a routine written in Splus to obtain slope and intercept information for a linear regression. Typically 15−21 data pairs of $1/\Phi_{obsd}$ vs viscosity data were in a sample in which 1000 iterations of the bootstrap were carried out. The subsequently calculated arrays of data were analyzed to yield mean values and variances of $1/\Phi_{pair}$, Φ_{pair}, slope, and k_{cP}/k_{dP}. (Each complete calculation was repeated three times.)

The static molecular volumes of the dimeric molecules were calculated using the computer program Steric[49] as previously described.[22]

Synthesis of $[(\eta^5\text{-}C_5H_5CH_2CH_2NH_3)_2Mo_2(CO)_6][NO_3]_2$. All of the following manipulations were performed under nitrogen. Cyclopentadienylethylamine ($CpCH_2CH_2NH_2$) was prepared as described in the literature[50] from the reaction of NaCp with 2 equiv of 2-bromoethylamine hydrobromide and purified by distillation under reduced pressure. A solution of $CpCH_2CH_2NH_2$ (9.01 g, 82.6 mmol) in THF was prepared by degassing $CpCH_2CH_2NH_2$ by one freeze−pump−thaw cycle and adding freshly distilled THF (100 mL). After the solution was cooled to −72 °C (dry ice/ethanol), 53 mL of *n*-butyllithium solution (1.6 M in cyclohexane, 84.8 mmol) was added dropwise through a pressure-equalizing addition funnel. The reaction mixture was allowed to warm to 0 °C and stirred further for 1 h followed by addition of $Mo(CO)_6$ (29.73 g, 82.6 mmol) under a counterflow of nitrogen. After the reaction mixture was refluxed for 48 h, it was cannulated into a concentrated aqueous solution (ca. 38 mL) of $Fe(NO_3)_3{\cdot}9H_2O$ (36.71 g, 90.9 mmol), which had been previously deoxygenated by purging nitrogen for 30 min and then cooled to 0 °C, resulting in the formation of a red precipitate. The reaction mixture was stirred for an additional hour and kept at 4 °C overnight. The precipitate was filtered in the air, washed with 20 mL of cold distilled water, transferred into a Schlenk flask, and then dried under vacuum. After removal of unreacted $Mo(CO)_6$ by sublimation onto a liquid nitrogen-cooled coldfinger under vacuum, the resulting solid was extracted with deoxygenated methanol under nitrogen in the dark several times until the extract was pale red. The extracted solution was filtered through a medium-porosity glass frit and concentrated under vacuum with minimal exposure to light. Diethyl ether (50 mL) was layered on top of this concentrated solution, and it was kept at 4 °C for 24 h. The product was isolated as a magenta-red solid following filtration and dried under vacuum for 5 h (6.21 g, 8.84 mmol, 21% yield). ^1H NMR (DMSO-d_6): δ 7.74[51] (s, br, 6H, $CpCH_2CH_2NH_3$, 5.72 (s, br, 4H, $CpCH_2CH_2NH_3$ anti rotamer[34c,52]), 5.62 (s, $CpCH_2CH_2\ NH_3$, anti and gauche rotamers), 5.40 (s, br, 4H, $CpCH_2CH_2NH_3$, gauche rotamer), 2.94 (t, 4 H, J = 7.2 Hz, $CpCH_2CH_2NH_3$), 2.66 (t, 4 H, J = 6.9 Hz, $CpCH_2CH_2NH_3$). UV−vis (CH_3OH): λ_{max} (ϵ, $M^{-1}\ cm^{-1}$), 505 (2080), 389 (20 100) nm.

Synthesis of $[(\eta^5\text{-}C_5H_4CH_2CH_2NHCO(CH_2)_3CH_3]_2Mo_2(CO)_6$ (1−1). The prior description[16] of this synthesis was relatively scant, so a detailed description follows. The complex was prepared by reacting $[(\eta^5\text{-}CH_4CH_2CH_2NH_3)_2Mo_2(CO)_6][NO_3]_2$ with a mixed anhydride derivative of valeric acid, which was prepared in situ. Deoxygenated valeric acid (156 μL, 1.43 mmol) and NEt_3 (284 μL, 2.04 mmol) were added by syringe to THF (10 mL), and the reaction mixture was stirred at 0 °C for 20 min. Addition of ethyl chloroformate (136 μL, 1.43 mmol) at 0 °C resulted in the formation of a Et_3NHC1 precipitate and the mixed anhydride derivative of valeric acid (Scheme 3). After the reaction mixture was stirred for 1 h at 0 °C, it was added by cannula to a suspension of $[(\eta^5\text{-}CH_4CH_2CH_2NH_3)_2Mo_2(CO)_6][NO_3]_2$ (480 mg, 0.68 mmol) in THF (20 mL) at 0 °C. Addition of concentrated aqueous K_2CO_3 (5 M; 0.7 mL,

3.50 mmol), which had previously been deoxygenated by purging with nitrogen for 20 min, resulted in a red homogeneous solution. The solvent was removed under vacuum, and the resulting red solid was washed with distilled water (20 mL) and dried under vacuum for 12 h. The resulting crude product (450.9 mg, 0.61 mmol, 90%) was further purified by column chromatography on silica gel using THF as eluent in the drybox. The desired eluted fractions were concentrated under reduced pressure, layered with hexanes, and kept at −30 °C for 12 h. The product was isolated as a red solid by filtration and then dried under high vacuum for 12 h (305 mg, 40.9 mmol, 60% yield). ^{1}H NMR ($CDC1_3$[53]): δ 5.52 (s, br, 2H $CpCH_2CH_2NH-$), 5.26 (s, br, 4H, $Cp$$CH_2CH_2-$), 5.16 (s, 4H, $Cp$$CH_2CH_2-$), 3.39 (m, 4H, $CpCH_2CH_2-$), 2.60 (t, 4 H, J = 7.2 Hz, $CpCH_2CH_2-$), 2.17 (t, 4 H, J = 7.8 Hz, $CpCH_2CH_2NHCOCH_2(CH_2)_2$, 1.60 (m, 4H, $CpCH_2CH_2NHCOCH_2CH_2$ CH_3), 1.34 (m, 4 H, $CpCH_2CH_2NHCO(CH_2)_2CH_2CH_3$), 0.92 (t, 6 H, J = 6.9 Hz, $CpCH_2CH_2NHCO(CH_2)_3CH_3$). ^{1}H NMR (DMSO-$d_6$): δ 7.89 (t, br, 2H, $CpCH_2CH_2NH-$), 5.62 (s, br, 4H, $Cp$$CH_2CH_2-$, anti rotamer), 5.54 (s, br, $Cp$$CH_2CH_2-$, anti rotamer), 5.46 (s, br, $Cp$$CH_2CH_2-$, gauche rotamer), 5.23 (s, br, 4H, $Cp$$CH_2CH_2-$, gauche rotamer), 3.16 (m, 4 H, $CpCH_2CH_2-$), 2.47[54] (m, 4 H, $CpCH_2CH_2-$), 2.05 (t, 4 H, J = 7.8 Hz, $CpCH_2CH_2NHCOCH_2(CH_2)_2CH_3$), 1.46 (m, 4H, $CpCH_2CH_2NHCOCH_2CH_2CH_2CH_3$), 1.23 (m, 4 H, $CpCH_2CH_2NHCO(CH_2)_2CH_2CH_3$), 0.85 (t, 6 H, J = 6.9 Hz, $CpCH_2CH_2NHCO(CH_2)_3CH_3$). IR (THF), ν(CO): 2008 (w), 1952 (vs), 1910 (s), 1897 (sh), 1884 (sh); ν(−CONH−): 1680 (w, br); ν(NH): 1535 (w, br), 1261 (vw) cm^{-1}. Anal. Calcd for $C_{30}H_{36}Mo_2N_2O_8$: C, 48.40; H, 4.87; N, 3.76. Found: C, 48.58; H, 4.67; N, 3.60.

Synthesis of [(η^5-$C_5H_4CH_2CH_2NHCO(CH_2)_8CH_3]_2Mo_2(CO)_6$ (2−2), [(η^5-$C_5H_4CH_2CH_2NHCO(CH_2)_{13}CH_3]_2Mo_2(CO)_6$ (3−3), and [(η^5-$C_5H_4CH_2CH_2NHCO(CH_2)_8CH_3]_2Mo_2(CO)_6$ (4−4). These complexes were prepared similarly to **1**−**1** by reacting [(η^5-$CH_4CH_2CH_2NH_3)_2Mo_2(CO)_6][NO_3]_2$ with the mixed anhydride derivatives of capric acid, pentadecanoic acid, and eicosanoic acid, respectively. Likewise, they were purified by the same method used to purify **1**−**1**. Complex **2**−**2**: yield, 46%. ^{1}H NMR ($CDC1_3$53): δ 5.52 (s, br, 2H, $CpCH_2CH_2NH-$), 5.26 (s, br, 4H, $Cp$$CH_2CH_2-$), 5.16 (s, 4H, $Cp$$CH_2CH_2-$), 3.39 (m, 4H, $CpCH_2CH_2-$), 2.60 (t, 4 H, J = 6.9 Hz, $CpCH_2CH_2-$), 2.16 (t, 4 H, J = 7.5 Hz, $CpCH_2CH_2NHCOCH_2(CH_2)_7CH_3$), 1.61 (m, 4H, $CpCH_2CH_2NHCOCH_2CH_2(CH_2)_6CH_3$), 1.26 (s, br, 24 H, $CpCH_2CH_2NHCO(CH_2)_2(CH_2)_6CH_3$), 0.88 (t, 6 H, J = 6.3 Hz, $CpCH_2CH_2NHCO(CH_2)_8(CH_3)$. ^{1}H NMR (DMSO-$d_6$): δ 7.88 (t, br, 2H, $CpCH_2CH_2NH-$), 5.62 (s, br, 4H, $Cp$$CH_2CH_2-$, anti rotamer), 5.53 (s, br, $Cp$$CH_2CH_2-$, anti rotamer), 5.46 (s, br, $Cp$$CH_2CH_2-$, gauche rotamer), 5.22 (s, br, 4H, $Cp$$CH_2CH_2-$, gauche rotamer), 3.15 (m, 4 H, $CpCH_2CH_2-$), 2.47[54] (m, 4 H, $CpCH_2CH_2-$, 2.03 (t, 4 H, J = 7.8 Hz, $CpCH_2CH_2NHCOCH_2(CH_2)_7CH_3$), 1.46 (m, 4H, $CpCH_2CH_2NHCOCH_2CH_2(CH_2)_6CH_3$), 1.23 (s, br, 24H, $CpCH_2CH_2NHCO(CH_2)_2(CH_2)_6CH_3$), 0.85 (t, 6 H, J = 6.9 Hz, $CpCH_2CH_2NHCO(CH_2)_3CH_3$). IR (THF), ν(CO): 2008 (w), 1952 (vs), 1910 (s), 1896 (sh), 1882 (sh); ν(−CONH−): 1680 (w, br); ν(NH): 1534 (w, br), 1250 (vw) cm^{-1}. Anal. Calcd for $C_{40}H_{56}Mo_2N_2O_8$: C, 54.30; H, 6.38; N, 3.17. Found: C, 54.17; H, 6.38; N, 3.31. Complex **3**−**3**: yield, 33%. ^{1}H NMR ($CDC1_3$[53]): δ 5.55 (s, br, 2H, $CpCH_2CH_2NH-$), 5.26 (s, br, 4H, $Cp$$CH_2CH_2-$), 5.16 (s, $Cp$$CH_2CH_2-$), 3.39 (m, 4H, $CpCH_2CH_2-$), 2.60 (t, 4 H, J = 7.2 Hz, $CpCH_2CH_2-$), 2.15 (t, 4 H, J = 7.8 Hz, $CpCH_2CH_2NHCOCH_2(CH_2)_{12}(CH_3)$, 1.60 (m, 4H, $CpCH_2CH_2NHCOCH_2CH_2(CH_2)_{11}CH_3$), 1.25 (s, br, 44 H, $CpCH_2CH_2NHCO(CH_2)_2(CH_2)_{11}CH_3$), 0.88 (t, 6 H, J = 6.6 Hz, $CpCH_2CH_2NHCO(CH_2)_{13}CH_3$). IR (THF), ν(CO): 2008 (w), 1952 (vs), 1910 (s), 1898 (sh), 1884 (sh); ν(−CONH−): 1680 (w, br); ν(NH): 1534 (w, br), 1261 (vw) cm^{-1}. Anal. Calcd for $C_{50}H_{76}Mo_2N_2O_8$: C, 58.59; H, 7.47: N, 2.73. Found: C, 58.37; H, 7.29; N, 2.93. Complex **4**−**4**: yield, 49%. ^{1}H NMR ($CDC1_3$[53]): δ 5.52 (s, br, 2H, $CpCH_2CH_2NH-$), 5.26 (s, br, 4H, $Cp$$CH_2CH_2-$), 5.16 (s, $Cp$$CH_2CH_2-$), 3.39 (m, 4H, $CpCH_2CH_2-$), 2.60 (t, 4 H, J = 7.2 Hz, $CpCH_2CH_2-$), 2.16 (t, 4 H, J = 8.1 Hz, $CpCH_2CH_2NHCOCH_2(CH_2)_{17}CH_3$), 1.56 (m, 4H, $CpCH_2CH_2NHCOCH_2CH_2(CH_2)_{16}CH_3$), 1.25 (s, br, 64 H, $CpCH_2CH_2NHCO(CH_2)_2(CH_2)_{16}(CH_3)$, 0.88 (t, 6 H, J = 6.9 Hz, $CpCH_2CH_2NHCO(CH_2)_{18}CH_3$). IR (THF), ν(CO): 2008 (w), 1952 (vs), 1910 (s), 1898 (sh), 1884 (sh); ν(−CONH−): 1680 (w, br); ν(NH): 1534 (w, br), 1262 (vw) cm^{-1}. Anal. Calcd for $C_{60}H_{96}Mo_2N_2O_8$: C, 61.84; H, 8.30; N, 2.51. Found: C, 61.82; H, 8.51; N, 2.51.

X-ray Crystal Structure Determination of [(η^5-$C_5H_4CH_2CH_2NHCO(CH_2)_3CH_3]_2$ $Mo_2(CO)_6$ (1−1). X-ray quality crystals of **1**−**1** were grown by slowly evaporating a THF solution of **1**−**1** under nitrogen. A crystal of dimensions 0.03 × 0.09 × 0.15 mm was sealed in a special glass capillary in the glovebag equipped with a microscope. The orientation parameters and cell dimensions were obtained from the setting angles of an Enraf-Nonius CAD-4 diffractometer for 25 centered reflections in the range $10° \leq \theta \leq 11°$. A summary of crystal data and the final residuals is in the Supporting Information as is a more extensive table including particulars of data collection and structure refinement.

Photochemical Reactions of Complexes 1−1, 2−2, 3−3, and 4−4. A stock solution consisting of 20% (v/v) $CC1_4$ in THF/tetraglyme was prepared. (For example, 10% (v/v) tetraglyme in THF was prepared by pipetting 20.00 mL of $CC1_4$ and 10 mL of tetraglyme into a 100.00 mL volumeteric flask and diluting with THF to the mark.) Additional THF (4−7 mL) was then added to ensure that four 25.00 mL aliquots and a solvent reference could be taken from the same stock solution. The masses of the samples were determined and the complexes transferred via multiple washings with the stock solution to volumetric flasks (25.00 mL) inside a darkened drybox. The concentrations of the samples were selected in order to afford absorbance readings between 0.7 and 1.5 at 546 nm. Aliquots (4.00 mL) of each compound in the solution of a specific viscosity were pipetted into each of three cuvettes (1 cm path length) equipped with a freeze−pump−thaw bulb (as a sidearm) and a stir bar and were then sealed. Each cuvette was degassed by four freeze−pump−thaw cycles and allowed to thermally equilibrate for at least 1 h and then placed in a cooled block at 23 ± 1 °C for 20 min before photolysis in the Merlin apparatus. The basic design of the Merlin apparatus for irradiations and quantum yield measurements has been discussed previously.[44] Light intensity was determined by actinometry using Aberchrome 540 in toluene ($\phi_{546} = 0.0470$)[45,46] and Reinecke's salt ($\phi_{545} = 0.282$).[47] Over a time period of 20 min, 401 intensity observations were collected, of which those 101 observations between 5 and 10 min were used for the determinations of quantum yields.

Acknowledgment is made to the National Science Foundation for the support of this work.

Supporting Information Available: Tables of crystallographic information, bond length and bond angles, nonbonded contact distances, calculated coordinates and thermal parameters for hydrogen atoms, anisotropic thermal parameters, torsion angles, least-squares planes, and a figure showing space-filling models of molecules **1**−**1** to **4**−**4**. This material is available free of charge via the Internet at http://pubs.acs.org.

References and Notes

(1) (a) Grassie, N.; Scott, G. *Polymer Degradation and Stabilisation*; Cambridge University Press: New York, 1985. (b) Guillet, J. *Polymer Photophysics and Photochemistry*; Cambridge University Press: Cambridge, 1985.
(2) Rabek, J. F. *Mechanisms of Photophysical Processes and Photochemical Reactions in Polymers*; Wiley: New York, 1987.
(3) Geuskens, G. In *Comprehensive Chemical Kinetics*; Bamford, C. H., Tipper, C. F. H., Eds.; Elsevier: New York, 1975; Vol. 14, pp 333−424.
(4) Guillet, J. E. In *Degradable Materials*; Barenberg, S. A., Brash, J. L., Narayan, R., Redpath, A. E., Eds.; CRC Press: Boston, 1990; pp 55−97.
(5) West, R.; Maxka, J. In *Inorganic and Organometallic Polymers*; Zeldin, M., Wynne, K. J., Allcock, H. R., Eds.; ACS Symposium Series 360; American Chemical Society: Washington, DC, 1988; Chapter 2.

(6) West, R. *L'actualite Chim.* **1984**, 64.
(7) West, R. *J. Organomet. Chem.* **1986**, *300*, 327.
(8) Hofer, D. C.; Miller, R. D.; Willson, C. G.; Neureuther, A. R. *SPIE, Adv. Resist Technol.* **1984**, *469*, 108.
(9) Ishikawa, M.; Nate, K. In *Inorganic and Organometallic Polymers*; Zeldin, M., Wynne, K. J., Allcock, H. R., Eds.; ACS Symposium Series 360; American Chemical Society: Washington, DC, 1988; Chapter 16.
(10) Yajima, S.; Hayashi, J.; Omori, M. *Chem. Lett.* **1975**, 931.
(11) Yajima, S. *Ceram. Bull.* **1983**, *62*, 893.
(12) Laine, R. M.; Blum, Y. D.; Tse, D.; Glaser, R. In *Inorganic and Organometallic Polymers*; Zeldin, M., Wynne, K. J., Allcock, H. R., Eds.; ACS Symposium Series 360; American Chemical Society: Washington, DC, 1988; Chapter 10.
(13) Gilead, D. In *Degradable Materials*; Barenberg, S. A., Brash, J. L., Narayan, R., Redpath, A. E., Eds.; CRC Press: Boston, 1990; pp 191−207.
(14) (a) Tenhaeff, S. C.; Tyler, D. R. *Organometallics* **1991**, *10*, 473−482. (b) Tenhaeff, S. C.; Tyler, D. R. *Organometallics* **1991**, *10*, 1116−1123.
(15) Tenhaeff, S. C.; Tyler, D. R. *Organometallics* **1992**, *11*, 1466−1473.
(16) Nieckarz, G. F.; Tyler, D. R. *Inorg. Chim. Acta* **1996**, *242*, 303−310.
(17) (a) Meyer, T. J.; Caspar, J. V. *Chem. Rev.* **1985**, *85*, 187. (b) Geoffroy, G. L.; Wrighton, M. S. *Organometallic Photochemistry*; Academic Press: New York, 1979.
(18) (a) Guillet, J. *Polymer Photophysics and Photochemistry*; Cambridge University Press: Cambridge, 1985; p 274. (b) The overall quantum yields decreased until a minimum value was reached, at which point a further increase in chain length did not decrease the quantum yield any further. At this point, presumably, segmental motion dominates molecular motion rather than center-of-mass diffusion, so an increase in chain length will have little effect on the efficiency of the reaction.
(19) Guillet, J. *Adv. Photochem.* **1988**, *14*, 91−133.
(20) (a) The concept of the "cage effect" was introduced by Franck and Rabinowitch[20b−d] in 1934 to explain why the efficiency of I_2 photodissociation was smaller in solution than in the gas phase. It was proposed that the solvent temporarily encapsulates the reactive I• atoms in a "solvent cage", causing them to remain as colliding neighbors before they either recombine or diffuse apart. This concept is illustrated by the reaction in Scheme 2. The point to note is that the formation of free radicals is preceded by the formation of a caged radical pair. (b) Franck, J.; Rabinowitch, E. *Trans. Faraday Soc.* **1934**, *30*, 120−131. (c) Rabinowitch, E.; Wood, W. C. *Trans. Faraday Soc.* **1936**, *32*, 138l−1387. (d) Rabinowitch, E. *Trans. Faraday Soc.* **1937**, *33*, 1225−1233.
(21) (a) Koenig, T.; Fischer, H. In *Free Radicals*; Kochi, J., Ed.; John Wiley: New York, 1973; Vol. 1, Chapter 4. (b) Koenig, T. In *Organic Free Radicals*; Pryor, W. A., Ed.; ACS Symposium Series 69; American Chemical Society: Washington, DC, 1978; Chapter 9.
(22) (a) Male, J. L.; Lindfors, B. E.; Covert, K. J.; Tyler, D. R. *Macromolecules* **1997**, *30*, 6404−6406. (b) Male, J. L.; Lindfors, B. E.; Covert, K. J.; Tyler, D. R. *J. Am. Chem. Soc.* **1998**, *120*, 13176−13186.
(23) More specifically and as discussed below, we showed that the results agreed with Noyes's theory of cage effects, which predicts that the ratio k_d/k_c is proportional to $m^{0.5}/r^2$, where m is the mass of the radical and r is its radius.
(24) More precisely, we showed that both the decrease in ϕ_{pair} (the quantum yield for the formation of the radical cage pair) and the increase in the cage effect (F_{cP}) contribute to the smaller overall quantum yields as the chain lengths increase. It was shown that the differences in ϕ_{pair} are largely responsible for the differences in Φ_{obs} at any particular viscosity. Thus, even at the highest viscosities, where the differences in the cage effects between the molecules are most pronounced, only about one-third of the difference in Φ_{obsd} between $(CpCH_2CH_2OSiR_3)_2Mo_2(CO)_6$ for R = Me and *n*-Hx is due to the difference in F_{cP} between the two molecules. The bulk of the difference is due to the differences in ϕ_{pair} between the two molecules.
(25) Covert, K. J.; Askew, E. F.; Grunkemeier, J.; Koenig, T.; Tyler, D. R. *J. Am. Chem. Soc.* **1992**, *114*, 10446−10448.
(26) The THF/tetraglyme solvent system was chosen so that the composition and polarities of the solvent and viscogen are extremely similar which will reduce the chance of selective solvation, a condition that could complicate the interpretations of the cage effect.
(27) It is important not to use polymeric viscogens because they can drastically alter the macroviscosity of a solution yet leave the microenvironment unchanged (i.e., they do not change the solvation of the solute). This comes about because large regions of the solvent are still unoccupied by the polymer. As an example of this phenomenon, Szwarc[28] showed that F_{cP} in the photolysis of $CF_3-N{=}N-CF_3$ in $CHCl_3$ did not change when 0.44% poly(ethylene oxide) was added to the solution, yet the macroviscosity increased about 6-fold. In a similar example, Grissom[29] altered the bulk viscosity of water using Ficoll-400, a polymer of sucrose and epichlorohydrin, but showed the viscosity surrounding the solute was relatively unchanged.
(28) Szwarc, M.; Wasserman, B. 160th National Meeting of the American Chemical Society, Chicago, IL, Sept 1970; Abstr. POLY 83.
(29) Grissom, C. B.; Chagovetz, A. M. *Z. Phys. Chem.* **1993**, *182*, 181−188.
(30) Laine, R. M.; Ford, P. C. *Inorg. Chem.* **1977**, *16*, 388−391.
(31) Previous work in supercritical fluids suggests that at low viscosities the yields of products are linear with respect to 1/viscosity and are also an extension of the same plots observed at room temperatures and pressures; see ref 32.
(32) Tanko, J. M.; Suleman, N. K.; Fletcher, B. *J. Am. Chem. Soc.* **1996**, *118*, 11958−11959.
(33) The $-CH_2CH_2-$ spacer can viewed as an electronic insulator that reduces any electronic variations caused by differences in n, the number of $-CH_2-$ groups. For a similar use of this strategy see: Hughes, R. P.; Trujillo, H. A. *Organometallics* **1996**, *15*, 286−294. Note that each molecule has an intense band at ≈390 nm in THF ($\epsilon \approx 20\,000$ cm^{-1} M^{-1}), assigned to the $\sigma \rightarrow \sigma^*$ transition, and a weaker band at ≈510 nm ($\epsilon \approx 2000$ cm^{-1} M^{-1}), assigned to a $d\pi \rightarrow \sigma^*$ transition. See ref 17a for further discussion of the electronic structures of these metal−metal bonded molecules.
(34) (a) Covert, K. J.; Male, J. L.; Tyler, D. R.; Weakley, T. J. R. *Acta Crystallogr., Sect. C* **1998**, *54*, 943−945. (b) Tenhaeff, S. C.; Tyler, D. R.; Weakley, T. J. R. *Acta Crystallogr., Sect. C* **1991**, *47*, 303−305. (c) Adams, R. D.; Collins, D. M.; Cotton, F. A. *Inorg. Chem.* **1974**, *13*, 1086−1090.
(35) From previous work in hexane,[22] the ϕ_{pair} values are as follows: R = Me, 0.61 ± 0.02; R = *i*-Pr, 0.56 ± 0.02; R = *n*-Pr, 0.55 ± 0.02; R = *n*-Hx, 0.46 ± 0.02.
(36) (a) Brookhart, M.; Green, M. L. H. *J. Organomet. Chem.* **1983**, *250*, 395. (b) Brookhart, M.; Green, M. L. H.; Wong, L.-L. *Prog. Inorg. Chem.* **1988**, *36*, 1−124.
(37) More precisely, it just has to be irreversible on the time scale of the cage processes, i.e., recombination and diffusion apart. As shown in Figure 4, the agostic species reacts with CCl_4 to from the trapped product, a reaction presumably preceded by cleavage of the Mo- - -H agostic bond. Thus, reversibility in the formation of the agostic species is suggested once the radicals are out of the solvent cage.
(38) (a) Yao, W.; Eisenstein, O.; Crabtree, R. H. *Inorg. Chim. Acta* **1997**, *254*, 105−111. (b) Crabtree, R. H.; Eisenstein, O.; Sini, G.; Peris, E. *J. Organomet. Chem.* **1998**, *567*, 7−11.
(39) Avey, A.; Weakley, T. J. R.; Tyler, D. R. *J. Am. Chem. Soc.* **1993**, *115*, 7706−7715.
(40) (a) Noyes, R. M. *J. Chem. Phys.* **1954**, *22*, 1349−1359. (b) Noyes, R. M. *Prog. React. Kinet.* **1961**, *1*, 129−160. (c) Noyes, R. M. *J. Am. Chem. Soc.* **1955**, *77*, 2042−2045. (d) Noyes, R. M. *J. Am. Chem. Soc.* **1956**, *78*, 5486-5490. (e) Noyes, R. M. *Z. Elektrochem.* **1960**, *64*, 153−156.
(41) This prediction is discussed in more detail in ref 68 of ref 22b above.
(42) Odian, G. *Principles of Polymerization*, 3rd ed.; Wiley-Interscience: New York, 1991; p 287.
(43) Perrin, D. D.; Armarego, W. L. F. *Purification of Laboratory Chemicals*, 3rd ed.; Pergamon: Oxford, 1988.
(44) Lindfors, B. E.; Nieckarz, G. F.; Tyler, D. R.; Glenn, A. G. *J. Photochem. Photobiol. A: Chem.* **1996**, *94*, 101−105.
(45) (a) Heller, H. G.; Langan, J. R. *J. Chem. Soc., Perkin Trans. 2* **1981**, 341−343. (b) Heller, H. G.; Langan, J. R. *EPA Newslett.* **1981**, *12*, 71−73. (c) Heller, H. G. *EPA Newslett.* **1993**, *47*, 44.
(46) (a) Heller, H. G. *EPA Newslett.* **1993**, *47*, 44. (b) Guo, Z.; Wang, G.; Tang, Y.; Song, X. *J. Photochem. Photobiol. A: Chem.* **1995**, *88*, 31−34. (c) Uhlmann, E.; Gauglitz, G. *J. Photochem. Photobiol. A: Chem.* **1996**, *98*, 45−49.
(47) (a) Adamson, A. W.; Wilkins, R. G. *J. Am. Chem. Soc.*. **1954**, *76*, 3379−3385. (b) Adamson, A. W. *J. Am. Chem. Soc.* **1958**, *80*, 3183−3189. (c) Adamson, A. W.; Sporer, A. H. *J. Am.*

Chem. Soc. **1958**, *80*, 3865−3870. (d) Wegner, E. E.; Adamson, A. W. *J. Am. Chem. Soc.* **1966**, *88*, 394−404.
(48) Efron, B.; Tibshirani, R. J. *An Introduction to the Bootstrap*; Chapman and Hall: New York, 1993.
(49) The computer program Steric was written by B. Craig Taverner, Department of Chemistry, Witwatersrand, Private Bag 3, WITS 2050, Johannesburg, South Africa.
(50) Nieckarz, G. F.; Litty, J. J.; Tyler, D. R. *J. Organomet. Chem.* **1998**, *554*, 19−28.
(51) The chemical shift for the ammonium proton varies slightly depending on the concentration (δ 7.74−7.81 ppm). As discussed in the text, there is no IR evidence for intra- or intermolecular hydrogen bonding; thus, the shift is not thought to be caused by hydrogen bonding.
(52) (a) Adams, R. D.; Cotton, F. A. *Inorg. Chim. Acta* **1973**, *7*, 153−156.
(53) The NMR sample was prepared in the dark and the spectrum obtained immediately in order to prevent any photochemical reaction with the solvent.
(54) This peak is obscured by deuterated solvent peaks.
(55) White, D.; Coville, N. J. *Adv. Organomet. Chem.* **1994**, *36*, 95−158.

MA990074Z